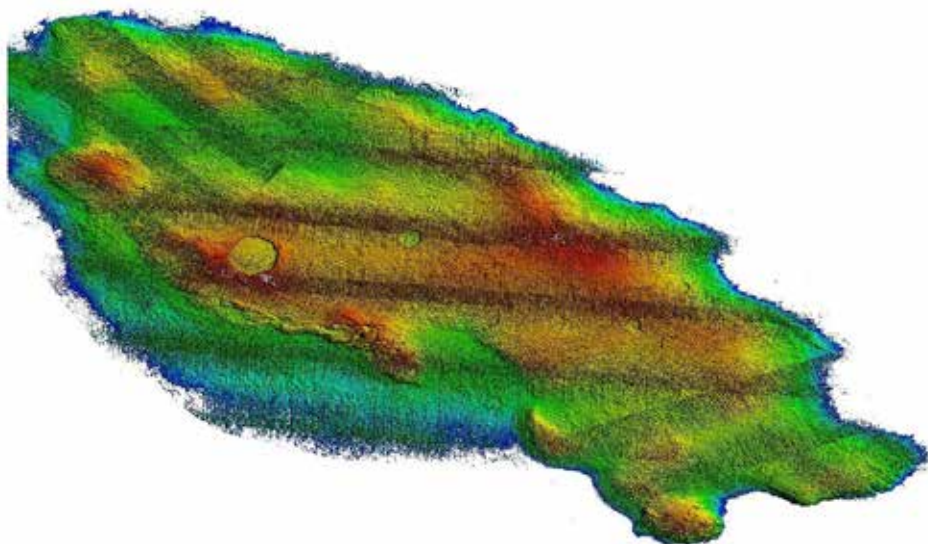


Pivot II

Constructs for an Environmental Understanding



Sikka l-Bajda Dolines

Underwater dolines identified through ERDF156 in 2012

GEO (WGS84) (14.3921986161, 36.0020301927) - -22.3 m,
36° 00' 07.3087" N, 14° 23' 31.9150" E

CHAPTER 7

Improving Weather Forecasts by Updating the Surface Boundary Conditions of a Numerical Weather Prediction Model for the Maltese Islands

Andrew Agius, Charles Galdies, Alannah Bonnici and Joel Azzopardi

Introduction

Multiple sectors of modern society have become dependent on accurate and regular weather forecasts. These allow them to make strategic and informed decisions in order to preserve and maintain their assets. Weather forecasts have also become an integral part of various systems and services, such as Decision Support Systems and Early Warning Systems, all of which play a crucial role in modern societies.

Numerical weather prediction (NWP) models are used to accurately compute synoptic weather conditions. One of the most commonly used NWP atmospheric simulators is the Weather Research and Forecasting (WRF) model (Lu, Zhong, Charney, Bian, & Liu, 2012; Evan, Alexander, & Dudhia, 2012), (Evan, Alexander, & Dudhia, 2012); Giannaros, Melas, Daglis, Keramitsoglou, & Kourtidis, 2013)). This model is a collaborative design effort between research and operational meteorological communities. It offers a state-of-the-art system which is continuously maintained to represent this critical body of knowledge within the scientific community. The WRF model is freeware with a wide variety of applications and which can be transferred and downloaded onto a variety of platforms. It is often used for both research and operational applications (Skamarock, et al., 2008).

Before simulating atmospheric conditions, an NWP model must first be initialised. There are two main types of input datasets which are mandatory for the model to be capable of performing a skilful simulation of weather synopsis: Estimated low resolution atmospheric data, to be used as input to the system's differential equations (such as Global Forecast System data which may be freely downloaded from the National Oceanic and Atmospheric Administration's (NOAA) data archives), and geographical land use categories. The higher the resolution and accuracy of these initial conditions, the more skilful the output forecasts. WRF provides a default global dataset which identifies

geographically stable parameters. However, this land cover dataset, provided as part of the downloaded model default configuration, has a relatively low resolution. This causes inaccuracies that limit the skill of the model in accurately simulating weather conditions over the respective geographical area.

The purpose of this study was to improve the land use categories boundary conditions datasets for the Maltese Islands and identifying any improvements to weather forecasts made thereafter. Validation of the WRF model sensitivity with the improved land use dataset is done by comparing the default simulation configuration output to the output run with the improved land use categories. In order to quantitatively compare the skill of the forecasts, statistics are computed to quantify their error and bias. For this study to be a success an improvement in forecast accuracy had to be observed.

NWP Models and High Resolution Weather Forecasts

Advances in NWP were possible with improvements in computer technology that led to higher accuracy, better spatial resolution of model simulations, the ability to make predictions for longer periods and a wider diversity of environmental simulations. The information generated has numerous applications, such as the identification of developing extreme weather events for risk and disaster management (WMO, 2013). Other applications include military operations, climate change monitoring and forecasting, agricultural production, economic trends and scientific research (Chang, Peña, & Toth, 2013). NWP models are able to take into account a wide range of variables whilst analysing how they relate and influence each other, allowing for weather forecasts with a higher level of information (Coiffier, 2011).

High resolution data allows models to identify micro processes that influence the development of weather phenomena and their characteristics (Geertsema & Schreur, 2009). High resolution forecasts, whose resolution can range from 5 km to less than 1 km, offer a more realistic and accurate indication of meteorological developments for regional forecast (Montmerle, 2014). The WRF model is one such high resolution forecasting NWP model (NOAA, 2016). With the computational capacity used within the context of this study it was possible to push the horizontal resolution of the output down to 1 km.

The Influence of EO data on NWP

EO (Earth Observation) systems are instrumental in the scientific analysis of earth systems and improved environmental management. They provide the information required to monitor phenomena such as air pollution, oceanic salinity, meteorological developments and forest fires over long periods of time. The level of information

recorded is limited by the designed observation spatial resolution of the instruments used (ESA, 2014). In weather forecasting, EO data collected can be used to determine initial and boundary conditions for the NWP model being used. These conditions include atmospheric status and composition, radiation fluctuations and atmospheric interactions, boundary layer atmospheric interactions with the Earth surface, and topographic information that identifies elevation changes, surface type and terrain composition. EO data is also used by meteorologists as a means of validating forecast accuracy. Data variables, such as temperature or precipitation, are validated by comparing numerically generated forecasts with EO data. A statistical assessment can numerically establish the accuracy of the simulation (Coiffier, 2011).

An Overview of the WRF Model

The WRF model is one of the most modern and frequently used NWP models (Collins, et al., 2013). It is an open source software with which users may simulate future atmospheric conditions (WRF, 2004). The modelling process is split into several phases: preprocessing which includes initialisation of the model's differential equations, the computation equations and physics settings within the model itself, and post-processing where data is manipulated through external software packages so as to obtain information (WRF Users, 2014).

Preprocessing steps occur in the WRF Preprocessing System (WPS), which is made up of three executables (Table 1) that are controlled through a variable list file called namelist.wps and then run (Figure 1):

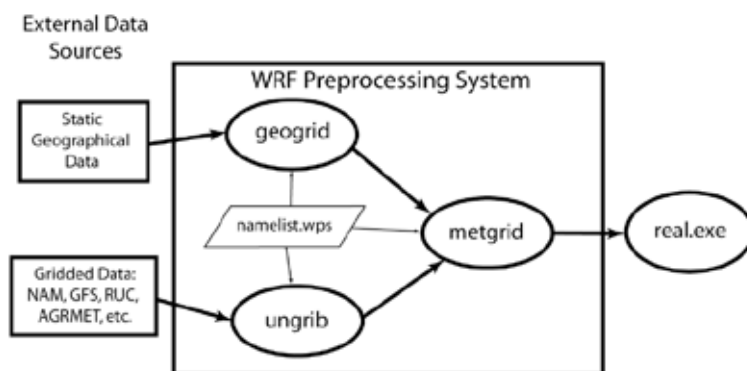
Table 1: The three WPS executables

WPS Executable	Function
geogrid	Defines the domains, grid resolution and applies static geographic data to the grid
ungrib	Converts meteorological input data from GRIB format to an intermediate format which can be interpreted by the model
metgrid	Interpolates the converted intermediary output files from ungrib executable onto the grid defined within the geogrid executable

Source: (NOAA, 2013).

Preprocessing prepares individual domains, or regions of Earth, for real data simulations in the WRF model (NOAA, 2013). The WPS is completed when the metgrid executable supplies its output to the WRF real program for further manipulation (Wang, et al., 2016).

Figure 1: The WPS process



Source: (Wang, et al., 2016)

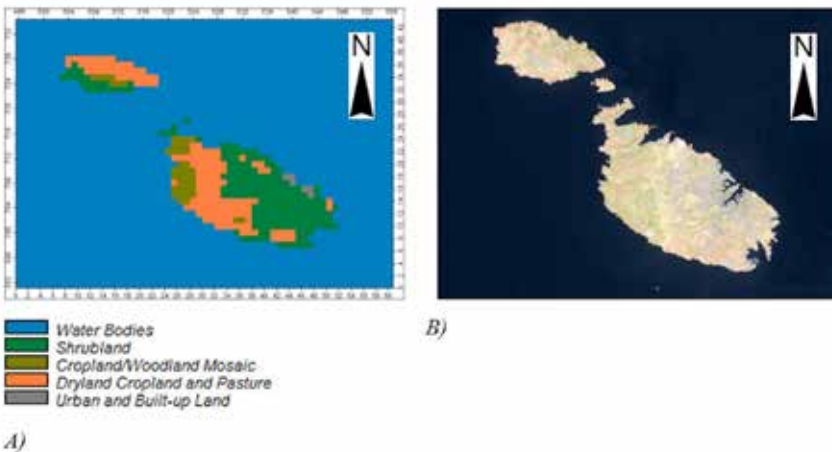
The following phase pertains to model initialisation, where the processed output from the WPS becomes the input supplied to the WRF model. The data is generated by a low resolution global forecast model and represents an estimation of the atmospheric conditions at 3 hourly time steps from the start of simulation. The supplied data is then prepared and processed for either a real or ideal simulations (Wang, et al., 2016).

Once initialised, the WRF model begins computing simulations. There are a number of different post-processing procedures available. Successfully completed simulations should undergo a validation procedure to quantify the skill of the forecasts. The user can also make use of tools to create visual representations of the output, such as time series graphs, forecast weather charts and 3D forecast representations (Wang, et al., 2016). Some of these data visualization tools come as add-ons to WRF or through external software packages such as MATLAB, SAGA, or ArcGIS. Another post-processing feature is called data assimilation for which the WRF model contains a package called WRF-DA. The very successful data assimilation process nudges the computed forecast variables with EO data to improve the estimated forecast (Skamarock, et al., 2008).

The WRF Geogrid Program and Land Use Categories

The WPS geogrid program establishes domains and grid resolution based on user specifications. This process initialises a number of variables at each grid point, including the longitude, latitude, surface albedo, terrain slope categories and elevations, and land use categories. Upon download the WRF model comes with default global datasets for each of these characteristic fields at 30 second, as well as 10, 5 and 2 minute resolutions (Wang, et al., 2016). One drawback of these datasets is that they may have low resolution and/or incorrect information. For example, the default land use categories dataset for the Maltese Islands (Figure 2a) limits the land use categories to four. On the other hand, an analysis of the Landsat 8 true colour image (Figure 2b) reveals a significantly higher number of categories and different distribution patterns.

Figure 2: The default WRF USGS 24-category Land Use Categories data set featuring the Maltese Islands (2a), generated with Saga version 2.1.1 and the true colour image of the Maltese Islands acquired via Landsat 8 on the 25th July 2014 at 09:36 hours (2b). Landsat Scene Identifier: LC81880352014206LGN00. Original image acquired from USGS EarthExplorer and edited with Picasa version 3.9.138.



WRF provides two default land use categories datasets: the USGS 24-category Land Use Categories, which is automatically selected by the geogrid program and the IGBP-Modified MODIS 20-category Land Use Categories. The latter, however, should only be used with the WRF Noah land surface model (Wang, et al., 2016). The USGS 24-category Land Use Categories follows the Anderson land-cover classification system published in 1976. This system splits classification into four levels based on data resolution, with Level I being used for data acquired through the LANDSAT project. This level is further

subdivided into the Level II classification system which deals with increased levels of information provided by higher data resolution. A detailed description of these land use categories can be found in 'A Land Use and Land Cover Classification System for use with Remote Sensor Data' (Anderson, Hardy, Roach, & Witmer, 1976).

EO Data Acquisition and Land Use Categorisation

For the purpose of this study an EO dataset for the Maltese Islands was downloaded from the USGS EarthExplorer website. This dataset was LANDSAT Scene Identifier: LC81880352014046LGN00, generated on the 15th of February 2014 at GMT 09:37 hours. LANDSAT 8 data was selected due to its relatively high quality, frequent passes over the same area, its reliability and its free to use policy. This image was selected because it was one of the few images where the Maltese Islands was not obscured by cloud cover (Figure 2b). It also provided a clear distinction between urban and rural areas due to the flourishing vegetation cover which is typical of the local mid-winter season.

The image bands used for this study have a 30 m resolution. LANDSAT 8 was selected as the data source due to its free to use policy and its image resolution of 15m, 30m and 100m (depending on the spectral channels selected). In addition, the LANDSAT data distribution policy ensures data dependability and compliance with the National Spatial Data Infrastructure (NSDI) managed by the US Federal Geographic Data Committee (FGDC) which, in turn, ensures data compatibility with a wide range of applications (Ryan & Freilich, 2008).

The default WRF dataset for the islands was also acquired and downloaded from the NOAA National Centers for Environmental Prediction (NCEP) Central Operations website (http://www.nco.ncep.noaa.gov/pmb/codes/nwprod/hwrf.v8.1.0/fix/hwrf_wps_geo/landuse_30s/), region 22801-24000.14401-15600 as per the WRF 1km resolution global grid system. This dataset was then visually compared to the LC81880352014046LGN00 image and deemed inaccurate. To improve this dataset, LANDSAT 8 image bands were analysed, processed and converted into the WRF geogrid format. This phase of the study was conducted with SAGA version 2.1.1 as it was freely available and due to previous experience with software usage.

The conversion process began with classifying the 30m resolution image in accordance to the USGS 24-category Land Use Categories with the Unsupervised Classification method. Bands B2, B3, B4 and B5 of image LC81880352014046LGN00 were imported into SAGA as raster images and cropped to show only the Maltese Islands (Table 2).

Table 2: A description of bands B2, B3, B4 and B5

Band	Description	Wavelength
Band 2 (B2)	Blue	0.45 - 0.51
Band 3 (B3)	Green	0.53 - 0.59
Band 4 (B4)	Red	0.64 - 0.67
Band 5 (B5)	Near Infrared (NIR)	0.85 - 0.88

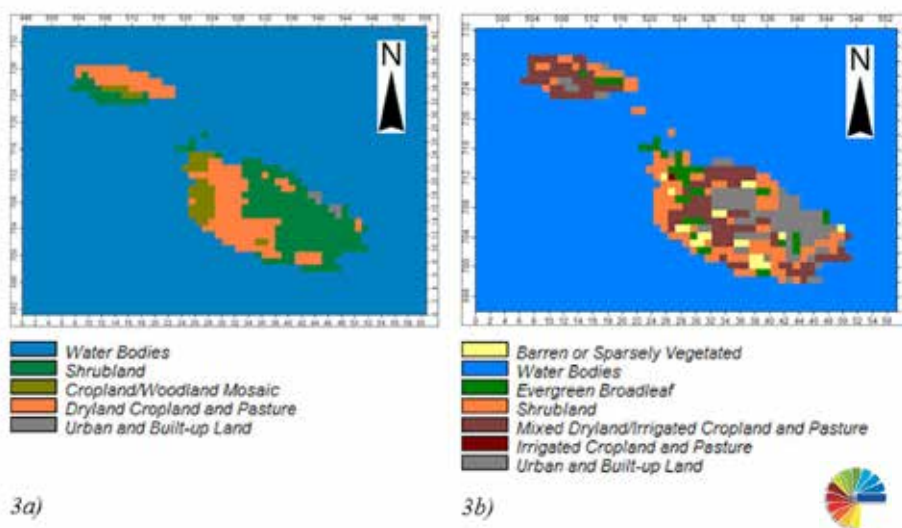
Source: (USGS, 2014).

This set of bands was selected to create a natural colour RGB image with enhanced vegetation cover (Butler, 2013). The statistical clustering method used for the unsupervised classification was the Hill climbing (Rubin 1967) method, with a limit of 24 clusters in accordance to the USGS 24-category Land Use Categories. The clustering process was followed by resampling which reduced the resolution from 30 m to 1 km in order to meet the data requirements of the geogrid.exe program (1 km resolution is considered as very high resolution in NWP research). Resampling was performed with the Majority interpolation method where a majority algorithm was used to determine the new 1 km resolution cell value based on the most popular 30 m resolution cell values (ArcGIS Resources, 2013).

Some regions, such as the urban areas and sea region, were automatically assigned more than one cluster due to multiple bands of light reflected from their surface. This resulted in 20 different clusters. Since the Maltese Islands have a limited number of applicable land uses, due to their geographical properties, it was necessary to change the assigned cluster values to those which gave the best representation according to the applicable USGS 24-category Land Use Categories. When determining the ideal category to be assigned reference was made to Google Earth imaging dated 15/04/2013. The Saga Change Grid Values module was used for this task with the default replace condition 'Grid value equals low value'. This module allows replacement of all the cells within a target cluster. The resultant data set contained 6 land use categories and the Water Bodies category. However, some areas were still deemed to be misrepresented, namely: The Valletta area, which was indicated as water bodies; and the Birżebbuġa area, where the sea within the mouth of the bay was indicated as urban and built-up land. To adjust this, the 'Change Cell Values' [interactive] module was used with the 'set constant value' method to properly categorise the grid cells.

Once this process was complete it was necessary to plot the improved categorisation image onto the original image, supplied by NOAA, with the Change Cell Values [interactive] module. The existing NOAA grid was altered by using the 'set constant value' method. Due to the projection differences between the two images it was also necessary to modify the improved image through image processing, before it was re-plotted onto the original one. The image was then converted into binary format by using the Export WRF Geogrid Binary Format module in 'Mercator' projection (Figure 3).

Figure 3: The default land use classification (3a) and the improved land use classification (3b) for the Maltese Islands at 1km resolution and according to the USGS 24-category Land Use Categories



Accuracy Assessment

To assess the accuracy of the product image classification, an error matrix was produced. The process involved taking 60 sample points, within the terrestrial boundaries of the archipelago, and comparing their actual composition (through Google Earth) with that generated by the unsupervised clustering. Point coordinates were identified with a random coordinate generator (www.geomidpoint.com/random). The area of influence was restricted to Malta (centre point at 35.9374960 latitude and 14.3754160 longitude), the number of points was limited to 250 and the maximum distance from the centre point set at 22 km.

An error matrix was then generated by comparing the observed land cover at each sampling point against the one generated with unsupervised clustering. A Producer's Accuracy assessment was conducted, followed by a User's Accuracy assessment and an Overall Accuracy assessment. While the Producer's accuracy provides an assessment of how well a certain area has been classified from a data producer point of view, the User's accuracy or reliability is indicative of the probability that a pixel classified on the map actually represents that category on the ground (Story and Congalton, 1986). On the basis of these two accuracies, the error matrix generates an Overall accuracy. This process was repeated for the default WRF 30s land use dataset in order to quantify the increase in accuracy of the improved land use categorisation scheme.

Running WRF and Generating a Real Scenario

Once the static geographical data had been updated, the WPS had to be re-run to produce new updated grids. This involved directing the WPS to the updated land use data files by updating their path in the namelist.wps file. The WPS section was completed by running the three executables and obtaining the updated output data files. The WRF model was re-run by directing it to the new updated WPS output files which were used as input.

Since the aim of this study was to determine whether improved boundary conditions would improve the skill of a NWP model output, a real forecast was generated using the improved statistical geographical land use data in order to compare it to real observation data. It was expected that the generated statistics would show an improvement in the accuracy and skill of the simulated forecast. The WRF core executables, real.exe and wrf.exe were executed and a wrf.out output file was produced.

Data validation techniques were applied to identify any differences between the observed data, the simulated forecast using the original geogrid data and the simulated forecast using the new geogrid data. Visual representations of the data validation procedure were produced using MATLAB, namely time series plots for the final 3 datasets at the different stations where real observations were available. Real observation data was available from the following 8 Met Office weather stations: Dingli, Luqa airfield, Benghajsa, Birkirkara, Selmun, Valletta, Xaghra and Xewkija stations. The variables validated as part of this exercise were variable 'T' (which provides perturbation potential temperature) and variable 'RAINNC' (which provides accumulated total grid scale precipitation).

These time series also identified the root mean squared error (RMSE) and bias ratio of the forecast plot using the improved land use categories and the forecast plot using

the default scheme. The RMSE value provides an indication of the overall forecast offset from the overall observed trend (the closer an RMSE value is to 0, the more accurate the forecast is). On the other hand, the bias ratio provides an indication of how much the forecast values vary from the observed data, with the observed data having a bias ratio value of 1. These overall indications are based on the average RMSE or bias ratio generated by each hourly forecast.

Improving the WRF 30s Land Use Categories for the Maltese Islands

The land cover classification identified the different types and distribution of terrestrial features that affect the local climate, such as vegetation, urban and agricultural land cover. Depending on their properties, these land cover types have an influence on the local humidity, temperature, evaporation, evapotranspiration, albedo and wind profiles. These influences are taken into account by the WRF model numerical calculations. Therefore, the accuracy of the land cover categories that is supplied to the model influences the model output accuracy. The default WRF 30s land use classification dataset for the Maltese Islands was limited in terms of the categories assigned and their distribution. Not only were categories assigned incorrectly, they were also distributed inaccurately. An error assessment based on a 60-point sample revealed an overall accuracy of 10%. On the other hand, the improved land use classification had an overall accuracy of 70%.

WRF Simulation Output Analysis

The precipitation and temperature time series plots showing the default and updated outputs, as well as observations for the 8 meteorological stations between 24/10/2010 at 00:00hrs and 26/10/2010 at 00:00hrs, identified changes in the RMSE and the bias ratio of the forecast plots. The results show that the improved land use classification led to an overall improvement in forecasting accuracy. The average precipitation onset forecast accuracy (Figure 4) was improved by 1.12% while the average precipitation quantity forecast (Figure 5) was improved by 3.35%. The average forecasted onset of the temperature fluctuation (Figure 6) was improved by 3.04% and the average predicted temperature values (Figure 7) were improved by 0.17%. The lack of significant improvement can be attributed to the numerical settings that were not adjusted to take into account the improved boundary conditions. By adjusting the default settings one may be able to compensate for the increased bias ratio and improve the overall accuracy. The inaccuracy level can also be reduced by improving other boundary conditions, such as terrain slope categories and elevations, surface albedo properties and soil categories. Since the land use categorisation was the only dataset improved, a number of discrepancies may have developed between this dataset and the remaining terrestrial boundary conditions.

It is also interesting to note that changes in RMSE value accuracy did not always correspond to changes in the bias ratio when applying the improved land use classification. While this occurred only once (13%) for surface temperature forecasts, in precipitation forecasts 63% of the outputs for the group of stations (1 per station) showed either an improved RMSE accuracy but a decreased bias ratio accuracy or vice versa. Further in-depth analysis which refers to the identification and application of more suitable numerical schemes embedded, but not active, within the WRF model is therefore required.

Figure 4: The precipitation onset forecast RMSE value of the outputs using the default and updated land use classification for each of the stations, and their relation to the ideal RMSE value (0).

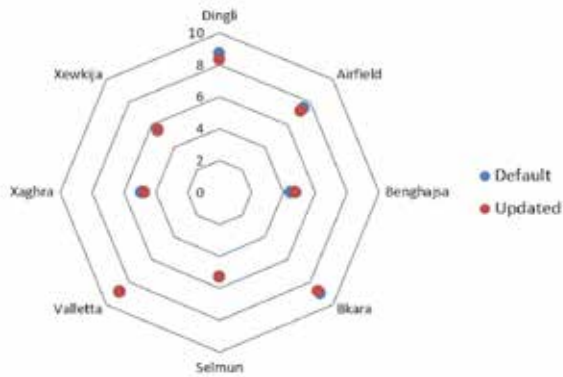


Figure 5: The precipitation quantity forecast bias ratio of the outputs using the default and updated land use classification for each of the stations, and their relation to the ideal bias ratio (1.0).

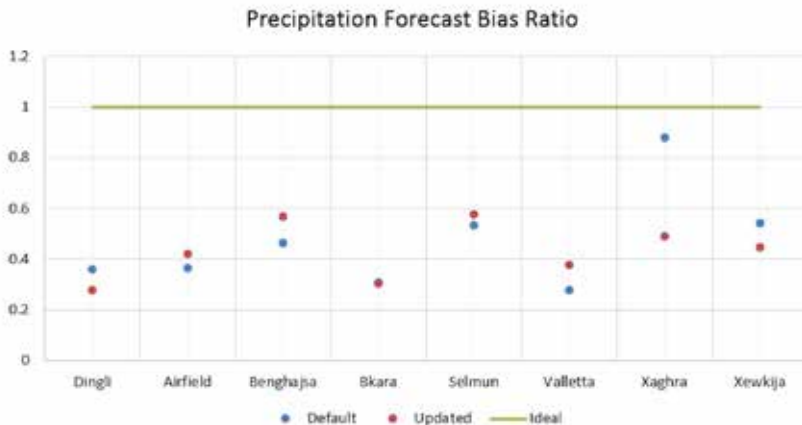


Figure 6: The surface temperature onset forecast RMSE value of the outputs using the default and updated land use classification for each of the stations and their relation to the ideal RMSE value (0).

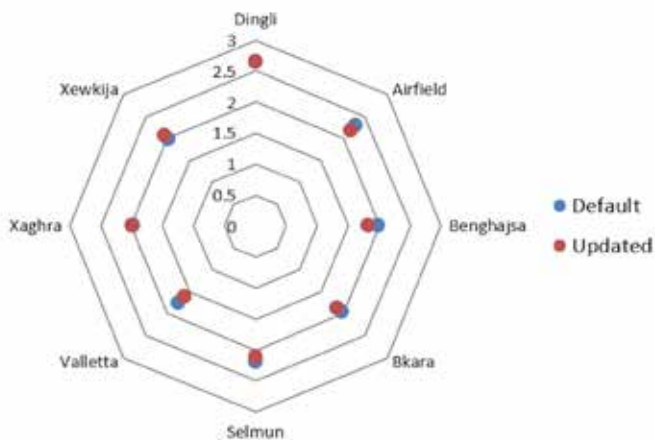
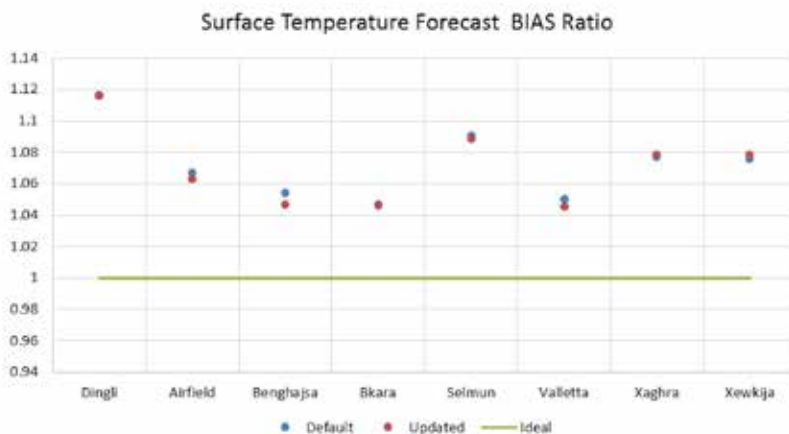


Figure 7: The surface temperature value forecast bias ratio of the outputs using the default and updated land use classification for each of the stations and their relation to the ideal bias ratio (1.0).



Limitations and Recommendations

The Mediterranean climate of the Maltese Islands means that the concentration of precipitation during the winter season causes the local vegetation to flourish, producing a greener land cover during the month of February. This was when the LANDSAT image was acquired. On the other hand, the summer season is dry resulting in a reduced vegetation cover (Aguado & Burt, 2007). In consequence, the differences in vegetation cover results in a discrepancy between the LANDSAT 8 image and the October land cover. Ideally, the terrestrial image selected provides the nearest representation of the conditions at the time of the simulation.

Further discrepancies may have been generated during the resampling process where, following the unsupervised classification procedure, the 30m resolution image was converted to 1km resolution. During resampling, pixel contamination may have occurred which would have had altered the land use categories distribution. These discrepancies contribute towards an increase in RMSE and bias ratio values of the WRF model output using the improved land use categorisation.

The model output may be further improved by making adjustments to the WRF model itself so as to find the best combination of numerical schemes responsible for skilful forecasting. It is also recommended that other default input datasets are updated. This would further exploit the improvements made by the improved land use categorisation. It is also recommended that WRF users improve the surface boundary conditions of their areas of interest in order to increase output accuracy.

As a continuation of this study, additional case studies are to be carried out in order to validate the impact of the improving the surface boundary conditions of NWP models.

Conclusion

The precipitation and temperature time series plots identified RMSE and bias ratio values of the default and updated WRF outputs revealed a minor improvement in forecast accuracy. The overall RMSE generated by the precipitation forecast indicates that the WRF output using the improved land cover categorisation boundary conditions produced a more accurate prediction in terms of precipitation onset. The bias ratio also indicates an improvement in the predicted precipitation quantity. Similarly, both the RMSE and bias ratio generated by the temperature time series plot indicated that the forecast generated using the improved boundary conditions was more accurate in terms of predicted temperature fluctuation onset and intensity.

One can therefore conclude that the improved land use categorisation led to an overall improvement in the WRF model 1km resolution output. However, further in-depth analysis is required to further exploit the information provided by the improved boundary conditions and thus increase the forecast accuracy. Furthermore, these analyses should identify and apply more suitable numerical schemes which are embedded, but not active, within the WRF model.

References

- Aguado, E., & Burt, J. E. (2007). *Understanding Weather and Climate* (4th ed.). New Jersey: Pearson Education, Inc.
- Anderson, J. R., Hardy, E. E., Roach, J. T., & Witmer, R. E. (1976). *A land use and land cover classification system for use with remote sensor data*. Washington: USGS. Retrieved from <http://landcover.usgs.gov/pdf/anderson.pdf>
- ArcGIS Resources. (2013, November 18). *ArcGIS Help 10.1*. Retrieved March 10, 2015, from ArcGIS Resources: <http://resources.arcgis.com/en/help/main/10.1/index.html#/00170000009t000000>
- Butler, K. (2013, July 24). *Band Combinations for Landsat 8*. Retrieved March 6, 2015, from ArcGIS Resources: <http://blogs.esri.com/esri/arcgis/2013/07/24/band-combinations-for-landsat-8/>
- Chang, E. K., Peña, M., & Toth, Z. (2013). International research collaboration in high-impact weather prediction. *Bulletin of the American Meteorological Society*, 94(11), 149-151. doi:10.1175/BAMS-D-13-00057.1
- Coiffier, J. (2011). *Fundamentals of numerical weather prediction*. Cambridge: Cambridge University Press.
- Collins, J., Farrimond, B., Anderson, M., Owens, D., Bayliss, D., & Gill, D. (2013). Automated Quality Assurance Analysis: WRF - A Case Study. *Journal of Software*, 8(9), 2177-2184. doi:10.4304/jsw.8.9.2177-2184
- ESA. (2014). *Observing the Earth*. Retrieved May 1, 2015, from ESA: http://www.esa.int/Our_Activities/Observing_the_Earth/How_does_Earth_Observation_work
- Evan, S., Alexander, M. J., & Dudhia, J. (2012). WRF simulations of convectively generated gravity waves in opposite QBO phases. *Journal of Geophysical Research: Atmospheres*, 117(12). doi:10.1029/2011JD017302
- Geertsema, G., & Schreur, B. W. (2009). The effect of improved nowcasting of precipitation on air quality modeling. *Atmospheric Environment*, 43(32), 4924-4934. doi:10.1016/j.atmosenv.2009.07.029
- Giannaros, T., Melas, D., Daglis, I. A., Keramitsoglou, I., & Kourtidis, K. (2013). Numerical study of the urban heat island over Athens (Greece) with the WRF model. *Atmospheric Environment*, 73, 103-111. doi:10.1016/j.atmosenv.2013.02.055

- Lu, W., Zhong, S., Charney, J. J., Bian, X., & Liu, S. (2012) WRF simulation over complex terrain during a southern California wildfire event. *Journal of Geophysical Research: Atmospheres*, Volume 117, Issue D5, CiteID D05125.
- Montmerle, T. (2014, July 17). *Statement of Guidance for High-Resolution Numerical Weather Prediction (NWP)*. Retrieved May 1, 2015, from World Meteorological Organization: <https://www.wmo.int/pages/prog/www/OSY/SOG/SoG-HighRes-NWP.pdf>
- NOAA. (2013, January 31). *WRF Portal Home*. Retrieved February 17, 2015, from NOAA Earth System Research Laboratory: Global Systems Division: <http://esrl.noaa.gov/gsd/wrfportal/>
- NOAA. (2016, May 1). *NSSL WRF 4 km grid initialized 00 UTC May 01 2016*. Retrieved May 1, 2016, from NOAA: <http://wrf.nssl.noaa.gov/>
- Ryan, B. J., & Freilich, M. H. (2008). *Landsat Data Distribution Policy*. USGS. Retrieved from http://landsat.usgs.gov/documents/Landsat_Data_Policy.pdf
- Story, M., and Congalton, R. (1986), Accuracy assessment: a user's perspective, *Photogramm. Eng. Remote Sens.* 52(3):397-399.
- Skamarock, W. C., Klemp, J. B., Dudhia, J., Gill, D. O., Barker, D. M., Duda, M. G., . . . Powers, J. G. (2008). *A description of the Advanced Research WRF version 3*. Boulder: National Center for Atmospheric Research. Retrieved from http://www2.mmm.ucar.edu/wrf/users/docs/arw_v3.pdf
- USGS. (2014, June 19). *Frequently Asked Questions about the Landsat Missions*. Retrieved March 6, 2015, from USGS science for a changing world: http://landsat.usgs.gov/band_designations_landsat_satellites.php
- USGS *EarthExplorer*. Retrieved from <https://earthexplorer.usgs.gov/>
- Wang, W., Bruyère, C., Duda, M., Dudhia, J., Gill, D., Kavulich, M., . . . Fossell, K. (2016). *ARW Version 3 Modeling System User's Guide January 2016*. National Center for Atmospheric Research. Retrieved from http://www2.mmm.ucar.edu/wrf/users/docs/user_guide_V3/ARWUsersGuideV3.pdf
- WMO. (2013). *Anticipated advances in Numerical Weather Prediction (NWP), and the growing technology gap in weather forecasting*. WMO. Retrieved from http://www.wmo.int/pages/prog/www/swfdp/Meetings/documents/Advances_NWP.pdf
- WRF. (2004). *The Weather Research & Forecasting Model*. Retrieved February 17, 2015, from The Weather Research & Forecasting Model: <http://wrf-model.org/index.php>
- WRF Users. (2014a, September 18). *User's Guide for the Advanced Research WRF (ARW) Modeling System Version 3.6*. Retrieved February 17, 2015, from WRF Users Page: http://www2.mmm.ucar.edu/wrf/users/docs/user_guide_V3/contents.html

